Setting Mechanism of a Biomimetic Bone Cement

Adriana Bigi,* Silvia Panzavolta, and Katia Rubini

Department of Chemistry "G. Ciamician", University of Bologna, 40126 Bologna, Italy

Received April 20, 2004. Revised Manuscript Received July 16, 2004

We have previously shown that gelatin addition to calcium phosphate bone cement improves its mechanical properties. To clarify the role of gelatin on the setting reaction of the cement, we carried out powder X-ray diffraction, DSC, TG, and SEM investigations on samples frozen after different times of soaking in simulated body fluid (SBF). The results indicate that the onset of the setting reaction is under the control of $CaHPO_4 \cdot 2H_2O$, which is contained in small amounts (5 wt %) in the α-tricalcium phosphate (α-TCP) cement, whereas the accelerating role of gelatin becomes the key factor just in a second step of the setting reaction. Gelatin controls the transformation of α-TCP into calcium deficient apatite (CDHA) and produces a composite biomimetic material with a close relationship between gelatin and CDHA crystals, which resembles that between collagen and apatite crystals in bone. With respect to the control cement, which does not contain gelatin, the gelatin−cement after setting exhibits reduced crystallinity, much smaller CDHA crystals, and a more compact microstructure, which can account for the improved mechanical properties.

Introduction

Calcium phosphate ceramics are of great interest for hard tissue repair due to their excellent biocompatibility and bioactivity properties.[1−3] The increasing demand of orthopaedic implant materials that can perfectly fit to a bone cavity, or that can be forged to the desired shape, leads to the development of calcium phosphate cements (CPCs).[4] Calcium phosphate cements are constituted of one or several calcium phosphates that, once mixed with a liquid phase, give a moldable paste. Within a few minutes, the paste sets because of the in situ formation of a solid calcium phosphate. The setting reaction provokes hardening of the paste through entanglements of the crystals of the precipitate.[5] The product of the setting reaction of CPCs is quite often calcium deficient hydroxyapatite, CDHA, which resembles the poorly crystalline carbonated apatite characteristic of bone and teeth. Since the first proposed formulation in the 1980s, a variety of cements based on different compositions have been proposed,[6−8] and the influence of a number of parameters, such as composition of the liquid phase, powder-to-liquid ratio, and Ca/P molar ratio, on the setting properties of the cements has been investigated.[6,9,10] α-Tricalcium phosphate, α-$Ca_3(PO_4)_2$ (α-TCP), is one of the main components of several apatitic cements. α-TCP displays a greater solubility than hydroxyapatite, and in aqueous solution, it undergoes hydrolysis through a mechanism that implies dissolution and successive precipitation of a more stable phase. The products of hydrolysis are dicalcium phosphate dihydrate ($CaHPO_4 \cdot 2H_2O$; DCPD), octacalcium phosphate ($Ca_8H_2(PO_4)_6 \cdot 5H_2O$; OCP), or apatite, depending on the working conditions.[11−14] At physiological values of pH and temperature, the product of hydrolysis is CDHA and the rate of the setting (hydrolysis) reaction can be modulated by addition of small amounts of other calcium salts.[13]

A material for hard tissue replacement must be able to create a bond with the host living tissue. It is suggested that this requirement is better fulfilled the more the synthetic material resembles the biological one in composition, structure, morphology, and crystallinity.[16] Mineralized tissues are composite materials where the presence of the organic matrix accounts for the peculiar structural, morphological, and mechanical properties. In particular, nucleation and growth of the inorganic crystals is under the strict control of the organic macromolecules.[17,18] Similarly, the use of poly-

* Corresponding author. Phone: +39 (051) 2099551; fax: +39 (051) 2099456; e-mail: adriana.bigi@unibo.it.

(1) Hench, L. L.; Wilson, J. *An introduction to bioceramics*; World Scientific: Hackensack, NJ, 1993.
(2) Suchanec, W.; Yoshimura, M. *J. Mater. Res.* **1998**, *13*, 94.
(3) Dorozhkin, S. V.; Epple, M. *Angew. Chem., Int. Ed.* **2002**, *41*, 3130.
(4) Bonher, M. *Injury* **2000**, *31*, D37.
(5) Fernández, E.; Gil, F. J.; Ginebra, M. P.; Driessens, F. C. M.; Planell, J. A.; Best, S. M. *J. Mater. Sci. Mater. Med.* **1999**, *10*, 177.
(6) Fernández, E.; Gil, F. J.; Ginebra, M. P.; Driessens, F. C. M.; Planell, J. A.; Best, S. M. *J. Mater. Sci. Mater. Med.* **1999**, *10*, 223.
(7) Khairoun, I.; Magne, D.; Gauthier, O.; Bouler, J. M.; Aguado, E.; Daculsi, G.; Weiss, P. *J. Biomed. Mater. Res.* **2002**, *60*, 633.
(8) Gbureck, U.; Grolms, O.; Barralet, J. E.; Grover, L. M.; Thull, R. *Biomaterials* **2003**, *24*, 4123.
(9) Driessens, F. C. M.; Boltong, M. C.; de Maeyer, E. A. P.; Wenz, R.; Nies, B.; Planell, J. A. *Biomaterials* **2002**, *23*, 4011.
(10) Driessens, F. C. M.; Boltong, M. G.; De Maeyer, E. A. P.; Verbeeck, R. M. H.; Wenz, R. *J. Mater. Sci. Mater. Med.* **2000**, *11*, 453.
(11) Elliott, J. C. *Structure and chemistry of the Apatites and Other Calcium Orthophosphates*; Elsevier: Amsterdam, 1994.
(12) Durucan, C.; Brown, P. W. *J. Mater. Sci. Mater. Med.* **2000**, *11*, 365.
(13) Durucan, C.; Brown, P. W. *J. Mater. Sci.* **2002**, *37*, 963.
(14) Bigi, A.; Boanini, E.; Botter, R.; Panzavolta, S.; Rubini, K. *Biomaterials* **2002**, *23*, 1849.
(15) Bigi, A.; Boanini, E.; Panzavolta, S.; Roveri, N. *Biomacromolecules* **2000**, *1*, 752.
(16) Jha, L. J.; Best, S. M.; Knoles, J. C.; Rehman, I.; Santos, J. D.; Bonfield, W. *J. Mater. Sci. Mater. Med.* **1997**, *8*, 185.
(17) Lowenstam, H. A.; Weiner, S. *On Biomineralization*; Oxford University Press: Oxford, 1989.

10.1021/cm049363e CCC: $27.50
Published on Web 08/26/2004

meric additives in CPCs formulation could allow us to modulate the characteristics of the final apatite crystals, as well as the properties of the CDHA/polymer cement. To this aim, we have previously investigated the effect of gelatin, a protein obtained by degradation of collagen, which is the main proteic component of bone tissue, on the setting properties of an α-TCP based cement.[19] The results indicated that the presence of gelatin accelerates the setting reaction and improves the mechanical properties of the biomimetic cements. The effect of gelatin is opposite to that verified for other polymeric additives, which quite often display a deleterious influence on the mechanical properties of calcium phosphate cements.[19] To clarify the mechanism of setting, and the role of gelatin on the properties of the final biomimetic cement, we have carried out a detailed physicochemical investigation on the setting reaction of the gelatin−cement.

Materials and Methods

α-TCP was obtained by a solid-state reaction of a mixture of $CaCO_3$ and $CaHPO_4 \cdot 2H_2O$ in the molar ratio of 1:2 at 1300 °C for 5 h.[14] Gelatin cement (Gel-C) was prepared using type A gelatin from pig skin (Italgelatine S.p.A.). α-TCP powder was added to gelatin aqueous solutions in the appropriate amount to obtain 15 wt % of gelatin in the composite material. The suspension was poured in Petri dishes, allowed to dry at room temperature, and then was crushed in an electric grinder and sieved through a 400-mesh sieve (38 μm). The specific surface area, evaluated by BET method using a Carlo Erba Sorpty 1750, was 1 m^2/g. The gelatin−cement powder (Gel-CP) was obtained by accurately mixing 5 wt % of DCPD ($CaHPO_4 \cdot 2H_2O$, Merck) with the gelatin/α-TCP. At variance, the powder (control cement powder: C-CP) used to prepare the control cement (C-C) contained α-TCP (95 wt %) and DCPD (5 wt %) without gelatin. The liquid phase (distilled water) and the cement powders were mixed in a mortar for 60 s to obtain a paste of workable consistency, using a liquid/powder ratio of 0.3 mL/g. Teflon molds were used to prepare cement cylinders 6 mm in diameter and 12 mm high. Soaking was performed in simulated body fluid (SBF) at 37 °C for different periods of time from 20 min up to 7 days.[15]

The specimens were removed from SBF after different times of soaking, demolded, and immediately immersed in liquid nitrogen for 10 min, to stop the setting reaction, and were ground in a mortar. For X-ray diffraction investigation, the samples were packed into recessed silicon slides. X-ray diffraction analysis was carried out by means of a Philips PW 1050/81-powder diffractometer equipped with a graphite monochromator in the diffracted beam. CuKα radiation was used (40 mA, 40 kV). The 2θ range was from 3 to 60° at a scanning speed of 0.75°/min. The relative amount of α-TCP conversion into CDHA was determined through the measurement of the integrated intensities of the reflections at 25.9 and 24.3° of 2θ, corresponding to the 002 reflection of hydroxyapatite and to the 131 reflections of α-TCP, respectively. The percentage of CDHA in the samples was determined from the value of $I_{002}/(I_{002} + I_{131})$ ratio, using a calibration curve obtained from weighted mechanical mixtures of hydroxyapatite and α-TCP.

To evaluate the coherence length of the CDHA crystals, further X-ray powder data were obtained in the relevant region of 2θ by means of step scans using a fixed counting time period of 10 s and a scan rate of 0.020°/step. The silicon standard peak 111 was used to evaluate the instrumental broadening.

Thermogravimetric analysis was carried out using a Perkin-Elmer TGA-7. Heating was performed in a platinum crucible in air flow (20 cm^3/min) at a rate of 5 °C/min up to 800 °C. The samples weights were in the range of 5−10 mg.

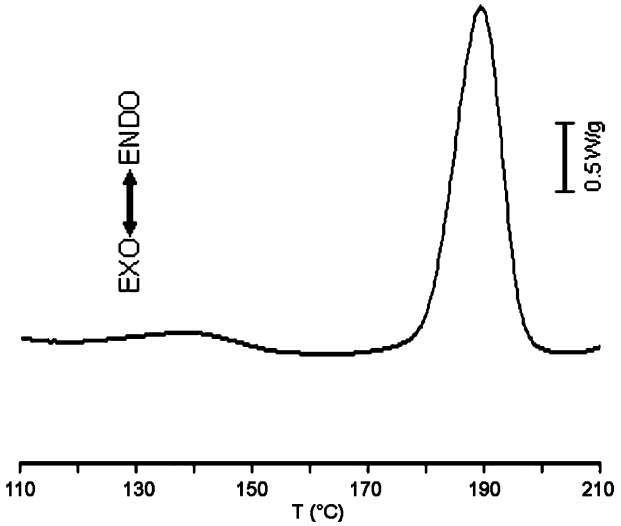

Figure 1. DSC curve of the control cement powder (C-CP).

Calorimetric measurements were performed using a Perkin-Elmer DSC-7 equipped with a model PII intracooler. Temperature and enthalpy calibration was performed by using high purity standards (*n*-decane, benzene, and indium). The measurements were carried out on known amounts of cements (3−4 mg of dried sample). Heating was carried out at 5 °C min^{-1} in the temperature range from 45 to 230 °C.

Morphological investigation of the fractured surfaces of the cement samples was performed using a Philips XL-20 Scanning Electron Microscope. The samples were sputter-coated with gold prior to examination.

Results

The DSC curve of the control cement (C-CP) exhibits two endothermic peaks due to DCPD (Figure 1). The first one, at about 130 °C, which is very small, has been ascribed to the removal of surface adsorbed (nonlattice) water from DCPD, whereas the second one corresponds to the thermal conversion of DCPD into anhydrous $CaHPO_4$ (DCPA), which occurs at about 190 °C.[22]The curve obtained for the gel−cement powder (Gel-CP) is quite similar, the only difference being the presence of a small broad endothermic peak at about 70 °C, due to gelatin denaturation.[21]

Figure 2a−g reports the DSC curves of the Gel-C samples frozen after different times of soaking in SBF. The comparison clearly shows the decrease of the peaks on increasing the soaking time; in particular, the area of the endothermic peak at about 190 °C, which is related to the enthalpy associated to the DCPD to DCPA transition, decreases and finally disappears for the samples soaked in SBF solution for 16 h. The relative amount of DCPD evaluated from the enthalpy values is reported in Figure 3 as a function of the aging time. A similar trend was obtained for the control cement.

The X-ray diffraction patterns of the cement powders display the reflections characteristic of α-TCP together with the diffraction reflections at 11.7 and 20.9° of 2θ, due to DCPD (Figure 4a). The intensities of the two peaks decrease with time so that they are barely

(18) Boskey, A. L. *Calcif. Tissue Int.* **1998**, *63*, 179.
(19) Bigi, A.; Bracci, B.; Panzavolta, S. *Biomaterials* **2004**, *25*, 2893.
(20) Dos Santos, L. A.; De Oliveira, L. C.; Rigo, E. C. S.; Carrodeguas, R. G.; Boschi, A. O.; DeArruda, A. C. F. *Bone* **1999**, *25*, 99.
(21) Landin, M.; Martinèz-Pacheco, R.; Gomèz-Amoza, J. L.; Souto, C.; Concheiro, A.; Rowe, R. C. *Int. J. Pharm*. **1994**, *103*, 9.
(22) Bigi, A.; Borghi, M.; Cojazzi, G.; Fichera, A. M.; Panzavolta, S.; Roveri, N. *J. Thermal Anal.* **2000**, *61*, 451.

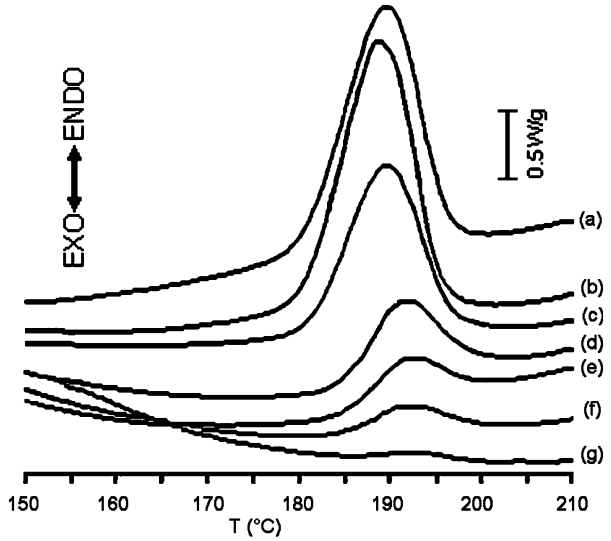

Figure 2. DSC curves of the gel−cement samples frozen after different times of aging in SBF: (a) 20 min; (b) 1 h; (c) 2 h; (d) 4 h; (e) 6 h; (f) 8 h; and (g) 16 h.

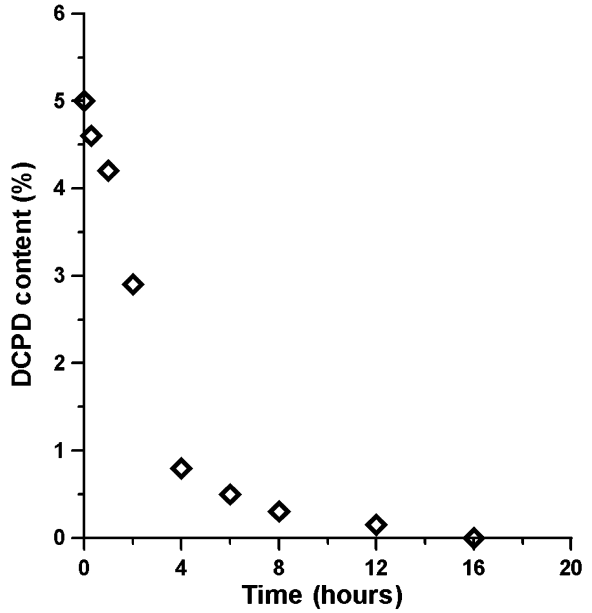

Figure 3. DCPD content of the gel−cement samples as a function of the soaking time in SBF.

appreciable in the X-ray pattern recorded after 2 h of aging, as is shown in Figure 4c. Furthermore, the X-ray pattern reported in Figure 4c shows the presence of a very small peak at 25.9° of 2θ, which corresponds to the 002 reflection of hydroxyapatite. The relative intensity of this reflection increases as a function of the soaking time, and hydroxyapatite is the only crystalline phase in the cements after 7 days of aging. The relative amounts of α-TCP and hydroxyapatite in the patterns of the samples soaked in SBF for increasing time periods have been evaluated using the calibration curve obtained through the analysis of the diffraction patterns of weighted mechanical mixtures of hydroxyapatite and α-TCP. The results obtained for the Gel-C and the C-C samples up to 48 h of aging are plotted in Figure 5. The increase of the relative amount of CDHA in the two cements is very similar up to 8 h of aging. A further increase of the soaking time provokes a drastic increase in the amount of α-TCP conversion into CDHA in the

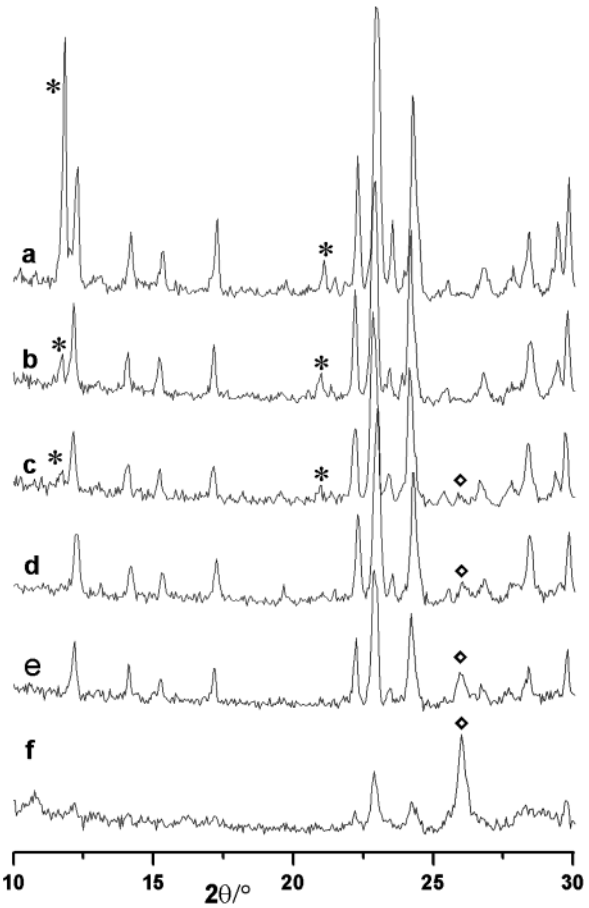

Figure 4. Powder X-ray diffraction patterns the gel−cement samples frozen after different times of soaking in SBF: (a) 5 min; (b) 20 min; (c) 2 h; (d) 8 h; (e) 16 h; and (f) 24 h. The main reflections of DCPD are indicated with (∗); the 002 reflection of CDHA is indicated with (◇).

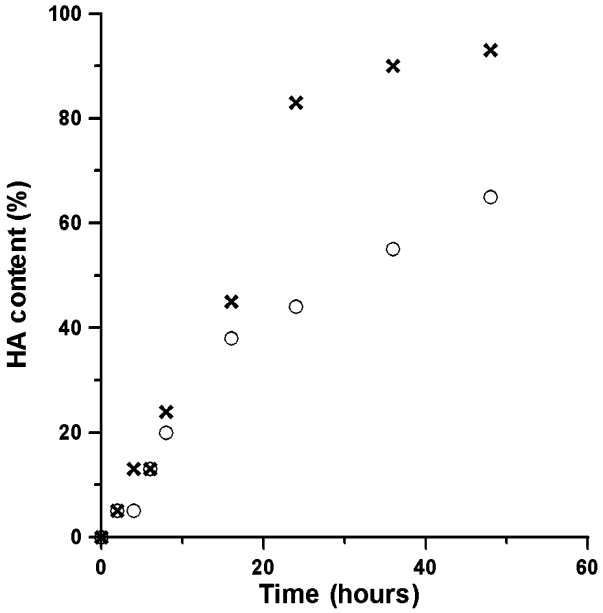

Figure 5. Relative amount of CDHA in the Gel-C (×) and in the C-C (○) samples as a function of the aging time in SBF.

Gel-C, whereas the transformation is slower in the C-C samples.

The lattice constants of the apatitic phase obtained after the setting of the two cements are very close and

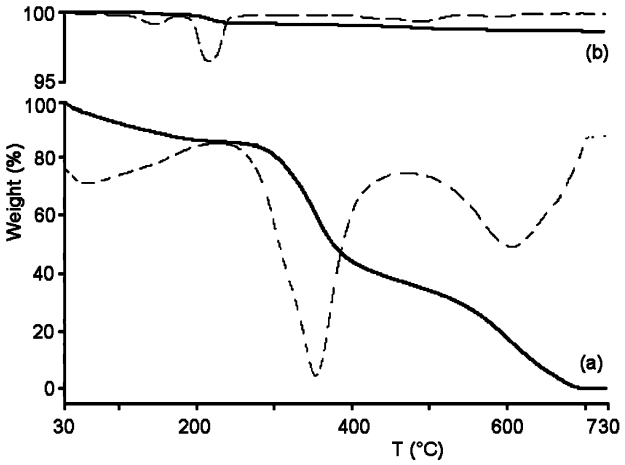

Figure 6. TG-DTG plots of (a) gelatin and of (b) the control cement powder (C-CP). TG curves are reported as full lines and DTG as dotted lines.

assume mean values of $a = 9.42(1)$ Å and $c = 6.88(1)$ Å. The line broadening of the hydroxyapatite 002 and 310 reflections was used to evaluate the length of the coherent domains (τ_{hkl}) along the *c*-axis and along a direction perpendicular to it. The τ_{002} and τ_{310} values calculated using the Scherrer equation[23] are 36.3(2) and 18.8(4) Å for C−C and 31.8(5) and 14.1(4) Å for Gel-C.

The thermogravimetric plot of gelatin (Figure 6a) displays three thermal processes: the first one occurs between 25 and about 250 °C, and it is due to loss of water; the second one between 250 and 450 °C involves gelatin decomposition; and the third one between 450 and 700 °C corresponds to the combustion of the residual organic component.[24] At variance, the TG-DTG plot of the C-CP displays just two very small weight losses between 100 and 250 °C, corresponding, respectively, to loss of adsorbed water and to the removal of structural water from DCPD (Figure 6b). The TG-DTG plot of the Gel-CP displays the contributions of DCPD and of gelatin. The DTG plots of the gel−cement samples frozen after different times of soaking in SBF are reported in Figure 7. In agreement with the DSC data, DCPD decreases as the aging time increases, so that even the peak at about 190 °C is no longer appreciable after 24 h of soaking (curves 7d,e). The total weight loss due to gelatin does not vary appreciably with time, suggesting that no significant amount of gelatin is released in the solution.

However, the peak temperature of the weight loss associated to the combustion of the residual organic components, which in pure gelatin is at 600 °C, shifts to lower temperature values as the soaking time in SBF increases. The peak temperature of the sample frozen just after the preparation of the cement (Figure 7a) decreases to about 550 °C, and it further decreases as the setting reaction proceeds. Moreover, the relative amount of weight loss associated to this peak with respect to the loss associated with the denaturation peak centered at 350 °C decreases on increasing time.

The SEM micrograph of Gel-C after 2 h of aging in SBF reported in Figure 8a shows the presence of a

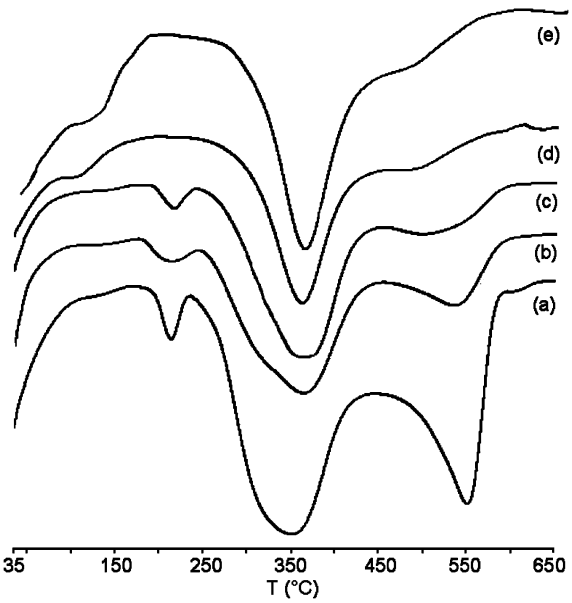

Figure 7. DTG plots of the Gel-C samples frozen after different times of soaking in SBF: (a) 5 min; (b) 20 min; (c) 2 h; (d) 24 h; and (e) 7 days.

number of α-TCP particles together with a huge platelike DCPD crystal. The image at greater magnification shown in Figure 8b puts into evidence the presence of smaller crystals that partly cover the space between the DCPD crystal and the nearby α-TCP particles. After 16 h of aging, the morphology of the cement-fractured surface appears completely modified into a much more compact microstructure, as shown in Figure 8c,d. Figure 9 reports the fractured surface of the control cement (a) and of the gel−cement (b) after 7 days of aging in SBF. The surface of C−C appears covered with entangled platelike crystals and exhibits several pores. At variance, the Gel-C fractured surface is compact and made up of very small crystals.

Discussion

The results of this paper put into evidence that the properties of gelatin-containing cements are greatly influenced by the interaction occurring between gelatin and inorganic crystals during the setting reaction. The inorganic component of the cement is α-TCP enriched with a small amount of DCPD. The presence of DCPD inside the cements can be easily detected through DSC analysis thanks to the endothermic peak at about 190 °C, which corresponds to the transition of DCPD into the anhydrous form, DCPA. The energy calculated from the peak integration is directly proportional to the amount of DCPD in the sample.[25] Therefore, the enthalpy value can be used for a quantitative determination of the amount of remaining DCPD in the cement samples frozen after different time of soaking in SBF. The plot of the amount of DCPD as a function of time reported in Figure 3 indicates that DCPD decreases exponentially as the setting reaction proceeds. The transformation of DCPD into CDHA, which is known to occur directly in the presence of the basic α-TCP, without involving DCPA formation,[13] starts soon after

(23) Alexander, L. E. *X-ray diffraction methods in polymer science*; Wiley- Interscience: New York, 1969.

(24) Bigi, A.; Cojazzi, G.; Koch, M. H. J.; Pizzuto, G.; Ripamonti, A.; Roveri, N. *Int. J. Biol. Macromol.* **1991**, *13*, 110.

(25) Boudeville, P.; Serraj, S.; Leloup, J. M.; Margerit, J.; Pauvert, B.; Terol, A. *J. Mater. Sci. Mater. Med.* **1999**, *10*, 99.

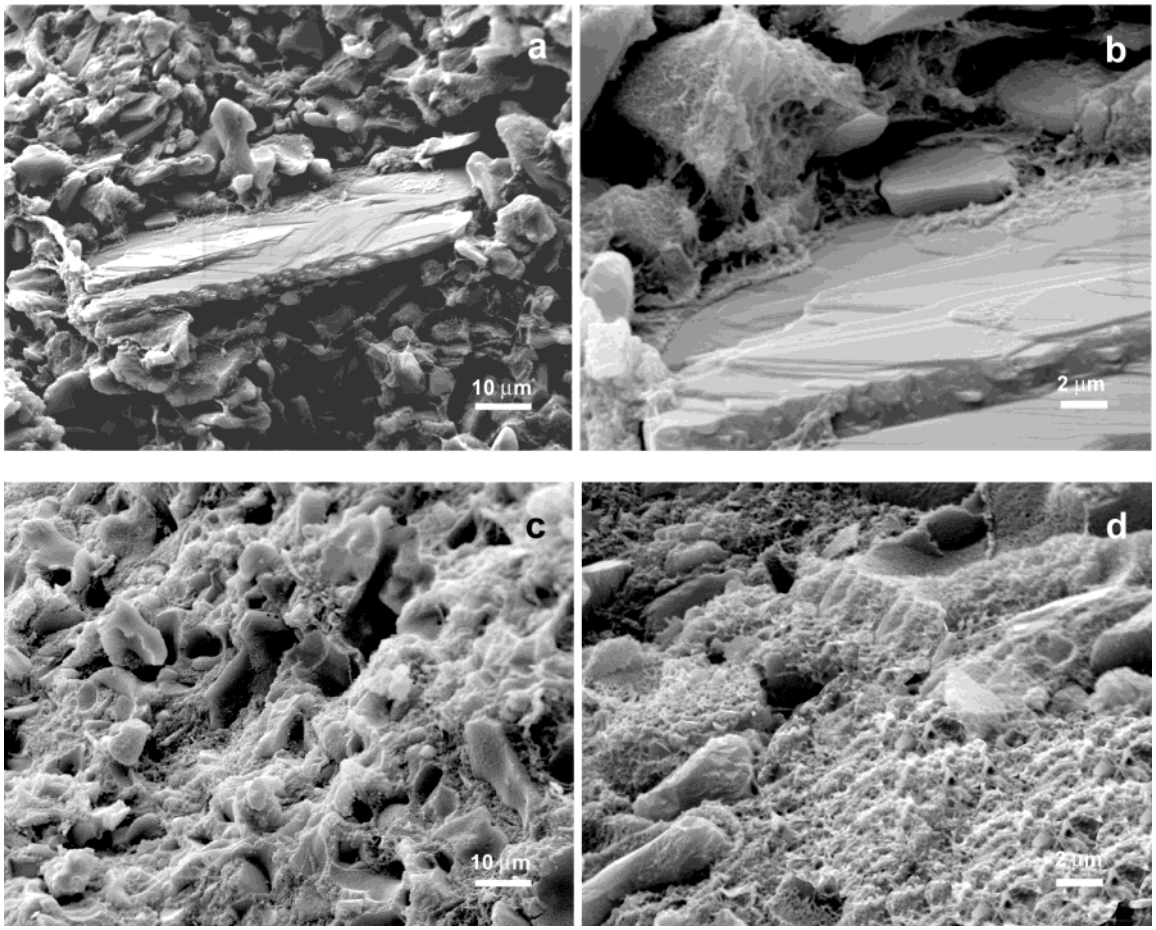

Figure 8. SEM micrographs of the fracture surfaces of the Gel-C samples after soaking in SBF for (a and b) 2 h and (c and d) 16 h.

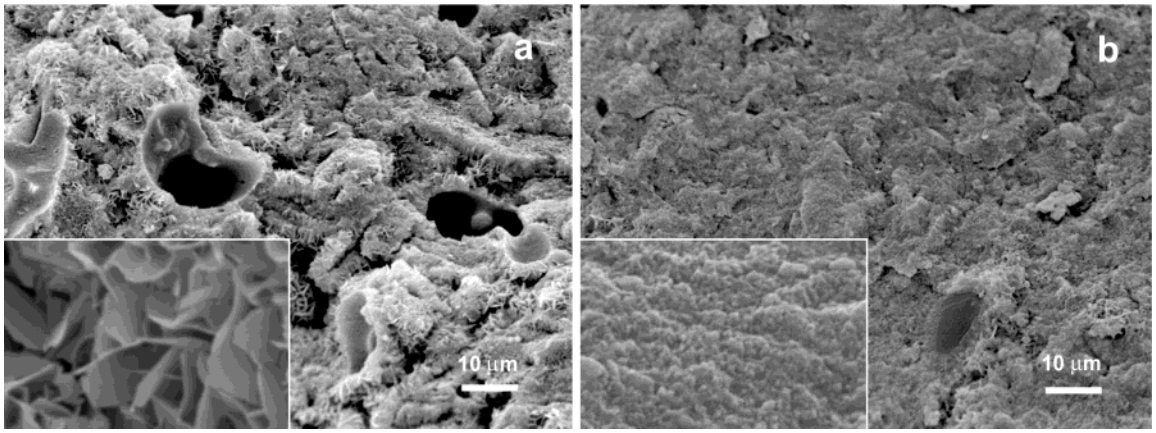

Figure 9. SEM micrographs of the fractured surfaces of (a) C-C and (b) Gel-C samples after aging in SBF for 7 days. The images in the inserts have been enlarged by a factor of 6.5.

the immersion of the cements in the SBF solution, and most of DCPD has already reacted when the first appreciable amount of CDHA can be evaluated from the X-ray powder patterns. It is worthwhile to remember that the sensitivity of the DSC technique is greater than that of the powder X-ray diffraction. As a matter of fact, although DCPD in the cement powders is well-evidenced by the presence of the two reflections at 11.7 and 20.9° of 2θ (Figure 4a), the rate of decrease of their relative intensities as a function of the soaking time in SBF is much faster than that of the characteristic endothermic peak in the DSC plot. The increase of the relative amount of CDHA during the first hours of the setting reaction is similar for Gel-C and C-C, but at longer soaking times, it results significantly greater in the Gel-C samples than in the C-C ones. These data confirm that gelatin accelerates the setting reaction of the cement[19,26] and reveal that the accelerating role of gelatin becomes very important just in a second step of the setting reaction. On the other hand, the onset of the reaction seems to be under the control of DCPD, as

(26) Bigi, A.; Cantelli, I.; Panzavolta, S.; Rubini, K. *J. Appl. Biomater. Biomech.* **2004**, *2*, 81.

suggested also by the results of the SEM investigation, which show that the very first CDHA crystals appear on the surface of the DCPD crystals (Figure 8b).

In agreement with the results of DSC investigation, the DTG plots of the Gel-C samples frozen after different times of soaking in SBF show that the weight loss associated to the DCPD → DCPA transition decreases on increasing the soaking time. Furthermore, the plots appear significantly modified in the range of temperature 450−700 °C. Samples examined after relatively long soaking times, when the transformation into CDHA is almost complete, exhibit TG-DTG plots quite similar to those characteristic of biologically calcified samples, such as bone and calcified tendon, where the combustion peak appears just as a shoulder of the decomposition peak.[24,27] The variation of the Gel-C thermogram indicates a strong interaction between gelatin and inorganic component during the setting reaction that leads to CDHA formation and suggests that the relationship between gelatin and CDHA crystals in the aged cement is similar to that between collagen and apatite crystals in biological calcified tissues. The high solubility of gelatin in aqueous solution is well-known.[28] However, the relative amount of gelatin in the gel−cement does not decrease appreciably during soaking in SBF, most likely because its strong interaction with the inorganic crystals prevents gelatin release in the aging solution. Gelatin is obtained from collagen degradation, and although it lacks the fibrillar structure characteristic of collagen, gelatin still contains portions of collagen triple-helix molecules.[28] The close resemblance of gelatin to collagen, which is the main part of the extracellular bone matrix, suggests that gelatin can offer nucleation sites that are quite similar to those of the biological matrix, which can accelerate the precipitation of CDHA, with a consequent inhibition of crystal growth during the setting reaction. The inhibition of crystal growth is in agreement with previous results on the effect of gelatin on the in vitro crystallization of calcium phosphates.[29,30]Accordingly, both the degree of crystallinity and the dimensions of the CDHA crystals are affected by gelatin. As a matter of fact, the dimensions of the coherent length of the perfect crystalline domains of the apatitic crystals in the aged Gel-C samples are significantly smaller than those obtained for the C-C samples both along the 002 and the 310 directions. Furthermore, the results of the SEM investigation show that the mean size of the CDHA crystals in the aged-control cement is much greater than those in the gel−cement, which displays a finer and more compact microstructure. The platelike entangled crystals in C-C do not fill all the volumes and leave small voids or pores all over the cement (Figure 9a). At variance, the gelatin cement exhibited a fractured surface almost devoid of pores, where it is quite difficult to distinguish the crystals due to their small dimension (Figure 9b). This is in agreement with our previous data[26] that indicated a reduction of the total porosity, which is known to play an important role on the mechanical properties of the cement,[31,32]on increasing gelatin content of the cements.[26] The closely packed microstructure of the gel−cement can account for the significantly greater compressive strength of the gel−cement with respect to that of the control cement.[19,26]

Conclusions

The results of this study reveal that the setting reaction of the gel−cement occurs through a close interaction between gelatin and inorganic crystals that accelerates the transformation of α-TCP into CDHA, inhibits CDHA crystal growth, and prevents gelatin release into the solution, leading to a biomimetic composite cement with improved mechanical properties. The data suggest that the uses of gelatin, a biocompatible polymer already widely employed in the biomedical field, can be successfully extended to calcium phosphate bone cements.

Acknowledgment. This research was carried out with the financial support of MIUR and the University of Bologna (Funds for Selected Research Topics). K.R. carried out this research activity thanks to a fellowship awarded by the Italgelatine S.p.A.

CM049363E

(27) Bigi, A.; Cojazzi, G.; Panzavolta, S.; Ripamonti, A.; Roveri, N.; Romanello, M.; Noris Suarez, K.; Moro, L. *J. Inorg. Biochem.* **1997**, *68*, 45.

(28) Veis, A. *The Macromolecular Chemistry of Gelatin*; Academic Press: New York, 1964.

(29) Busch, S.; Schwarz, U.; Kniep, R. *Chem. Mater.* **2001**, *13*, 3260.

(30) Iijima, M.; Moriwaki, Y.; Takagi, T.; Moradian-Oldak, J. *J. Cryst. Growth* **2001**, *222*, 615.

(31) Barralet, J. E.; Gaunt, T.; Wright, A. J.; Gibson, I. R.; Knowles, J. C. *J. Biomed. Mater. Res.* **2002**, *63*, 1.

(32) del Real, R. P.; Wolke, J. G. C.; Vallet-Regi, M.; Jansen, J. A. *Biomaterials* **2002**, *23*, 3673.